Science of the Total Environment 974 (2025) 179208

Contents lists available at ScienceDirect

Science of the Total Environment

journal homepage: www.elsevier.com/locate/scitotenv

Inactivating facultative pathogen bacteria and antibiotic resistance genes in wastewater using blue light irradiation combined with a photosensitizer and hydrogen peroxide

Xiaoyu Cong [a], Carsten Ulrich Schwermer [b], Peter Krolla [a], Thomas Schwartz [a,*]

[a] Karlsruhe Institute of Technology (KIT), Institute of Functional Interfaces (IFG), Hermann von Helmholtz Platz 1, 76344 Eggenstein-Leopoldshafen, Germany
[b] Norwegian Institute for Water Research (NIVA), Økernveien 94, 0579 Oslo, Norway

HIGHLIGHTS

- Antimicrobial blue light (aBL) reduced ESKAPE bacteria and antibiotic resistances.
- Photosensitizers and oxidative agents significantly enhanced decontamination.
- Gram-positive bacteria were more sensitive to aBL irradiation.
- Bacteria carrying *erm*B, *tet*M, *sul*1, or bla_{VIM} genes showed the highest reductions.
- About 13 DNA lesions per 10 kb were detected contributing to bacterial inactivation.

GRAPHICAL ABSTRACT

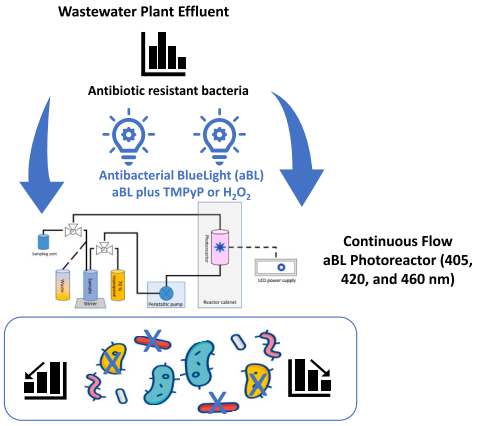

ARTICLE INFO

Editor: Daniel Wunderlin

Keywords:
Antimicrobial BlueLight (aBL)
Antibiotic resistances
Continuous flow photoreactor
DNA lesions
Photoenhancers
Wastewater disinfection effectiveness

ABSTRACT

The effectiveness of antimicrobial blue light (aBL) irradiation in eliminating ten clinically significant antibiotic resistance genes (ARGs) and four taxonomic marker genes of the WHO-priority ESKAPE bacteria group from wastewater treatment plant (WWTP) effluent was examined. Experiments were conducted using an LED-driven continuous-flow photoreactor operating at wavelengths of 405 nm, 420 nm, and 460 nm. Irradiation with aBL alone was insufficient for effectively inactivating or eliminating ESKAPE bacteria and clinically relevant ARGs. The addition of the porphyrin-based photosensitizer TMPyP (10^{-6} M) or the oxidative agent H_2O_2 (1 mM) resulted in several $\log_{10}$ unit reductions of facultative pathogenic bacteria (FPB), their taxonomic gene markers, and target ARGs. However, the additional effects of TMPyP and H_2O_2 were only noticeable in conjunction with aBL irradiation, as they were ineffective without it.

The reduction of the different FPB and ARGs in WWTP effluents was analyzed using culturing and qPCR together with living/dead discrimination. Different FPB and ARGs showed varying susceptibility to aBL-mediated irradiation. Among the FPB, enterococci were the most sensitive, while among the ARGs bacteria carrying *erm*B,

* Corresponding author.
E-mail address: thomas.schwartz@kit.edu (T. Schwartz).

https://doi.org/10.1016/j.scitotenv.2025.179208
Received 5 December 2024; Received in revised form 19 March 2025; Accepted 20 March 2025
Available online 25 March 2025

*tet*M, *sul*1, and bla_{VIM} genes exhibited the strongest removal. This sensitivity may be due to the gene-carrying microorganism's response to aBL irradiation combined with TMPyP or H_2O_2. Additionally, molecular biology results revealed that aBL irradiation induced up to 13 lesions per 10 kb DNA, which is hypothesized to contribute to the acute inactivation effect and prevent regrowth by inhibiting DNA repair activities.

1. Introduction

The increasing prevalence of antimicrobial resistance (AMR) in clinical, veterinary, and environmental contexts poses a serious public health threat (Ahmed et al., 2024). Currently, the spread of antibiotic resistance and antibiotic residues in the aquatic environment is unregulated, with no limit values and no indicator systems for their detection exist, and significant knowledge gaps about antibiotic resistance, its evolution, dissemination, and associated health risks. In this context, the German BMBF-funded project HyReKa 'Hygienic-medical relevance and control of antibiotic-resistant pathogens in clinical, agricultural, and municipal wastewater and their significance in raw water' was carried out (https://www.ifg.kit.edu/downloads/HyReKA%20Abschlussbericht%20Oktober%202020.pdf).

This project compared conventional disinfection techniques like membrane filtration, ozone treatment, and UV irradiation for wastewater effluent decontamination targeting clinically facultative pathogenic bacteria (FPB) and antibiotic resistance genes (ARGs) by cultivation and qPCR. The findings highlighted the need for innovative decentral measures for wastewater decontamination.

The propose EU urban wastewater treatment directive (https://eur-lex.europa.eu/legal-content/EN/TXT/?uri=CELEX%3A52022PC0541), emphasizes the importance of antibiotic resistance within the European 'One Health Action Plan'. The directive, referencing the World Health Organisation (WHO), identifies wastewater as an important source of antibiotic agents, their metabolites, antibiotic-resistant bacteria (ARB), and resistance genes. Consequently, mandatory monitoring of antibiotic resistance in municipal wastewater and initiation of appropriate regulations are deemed necessary. Hence, infection management should prioritize preventing the dissemination and spread of ARB carrying clinically relevant ARGs discharged from critical sources like hospitals, nursing homes, and industrial livestock farming (Sib et al., 2019; WHO, 2019; Alexander et al., 2022). The misuse of antibiotics continues to drive the selection of antibiotic resistance selection and evolution in pathogenic bacteria, potentially leading to untreatable infections in the near future (O'Neil, 2014).

Hospitals are known as potent hotspots for the emergence and dissemination of AMR and associated gene pools through clinic-associated pathways (Sib et al., 2020, 2019), while WWTPs serve as a final control point for discharging wastewater-born ARGs into receiving aquatic environments. Decentralized upstream monitoring of wastewater from selected urban areas has been conducted earlier (Hembach et al., 2017; Alexander et al., 2020). Local wastewater treatment at hospitals was initialized at a few hospitals in Germany, Switzerland, and Netherland. Pharmafilter is one commercially available system, while other more compact solutions, that often are based on advanced treatment principles, such as membrane filtration, ozonation, and UV-treatment are in research and pilot-stage. Besides hospitals, retirement homes and slaughterhouses have been identified as significant sources of ARG discharges, often exhibiting higher levels than residential sewer systems (Cong et al., 2023; Alexander et al., 2020). Conventional treatment methods have proven ineffectual in eradicating ARB and ARGs. Primary treatment achieves only modest reductions (ARB: 0–1 log units, ARGs: 0.09–0.55 log units) (Hazra and Durso, 2022), while suboptimal sedimentation exacerbates their downstream dissemination. Moreover, secondary processes such as activated sludge may trap ARGs and ARB, inadvertently reintroducing them into environmental settings (Wang and Chen, 2020). Accordingly, the deployment of innovative advanced oxidative processes, particularly those light-based technologies are essential. Light-based wastewater disinfection employs various light sources to inactivate pathogens. Among these, UV disinfection remains predominant, inflicting irreparable damage to microbial nucleic acids without leaving chemical residues (Hazra et al., 2024). Emerging LED systems offer enhanced energy efficiency and durability (MacIsaac et al., 2024), while photocatalytic disinfection, which strengthen UV light with catalysts like titanium dioxide, being responsible for the decomposition of contaminants and the eradication of pathogens (Cong et al., 2024). Ozone can be generated by UV light and has strong disinfectant properties. It is often used in combination with other processes to increase the efficiency of disinfection. Besides these technologies, hydrogen peroxide (H_2O_2) is also a potent oxidant widely used in disinfection due to its ability to enhance antimicrobial effects while producing fewer by-products (Herraiz-Carboné et al., 2021; Garcez et al., 2011).

Our research focuses on the decentralized implementation of innovative, modular disinfection technologies. Such as aBL irradiation combined with photosensitizers (e.g., porphyrins) or oxidative agents (H_2O_2), to effectively curb the spread of AMR (Cong et al., 2023).

Treating wastewater at AMR hotspots can prevent contamination of larger wastewaters volumes downstream, thus, unburden WWTPs in the load of these contaminants. This strategy would support a more cost-effective treatment compared to central actions at WWTPs alone.

The novel application of aBL irradiation in the 400–470 nm range offers a sophisticated, strategy to combat AMR (Cong et al., 2023; Woźniak and Grinholc, 2022). aBL disinfection is based on the activation of endogen photosensitizers within bacterial cells by specific wavelengths of blue light. This activation triggers the production of reactive oxygen species (ROS), which are highly cytotoxic and lead to bacterial cell damage and death (Ngo et al., 2023; Leanse et al., 2022; Wainwright, 1998). The effectiveness of aBL treatment can vary significantly with changes in wavelength and dose (Huang et al., 2023). Endogenous porphyrins, critical chromophores in bacterial cells, act as inherent photosensitizers essential for photoinactivation (Maclean et al., 2009). We recently demonstrated that aBL in a static photoreactor holds significant potential for inactivating health-relevant FPB in polluted wastewater (Cong et al., 2023). In extension to the static photoreactor with small volumes of wastewater samples, this study is working with a continuous flow photoreactor using larger volumes of real WWTP effluent wastewater comparing the inactivation effectiveness for FPB and ARGs in a laboratory scaled reactor system. Here, three distinct LED wavelengths (i.e., 405, 420, and 460 nm) to assess their different inactivation effectiveness. The investigation used culturing and molecular biology techniques to evaluate the impact of aBL irradiation. The photodynamic porphyrin TMPyP (5,10,15,20-Tetrakis-(*N*-methyl-4-pyridyl)21,23-porphyrintetratosylate) (Figure S1) and the oxidizing agents H_2O_2 were added to enhance the aBL irradation effectiveness. We also aimed to confirm that bacterial DNA damage induced by aBL irradiation plus TMPyP or H_2O_2. Understanding the extent of DNA lesion formation is important for elucidating aBL inactivation mechanisms. DNA damages in wastewater irradiated with aBL were quantified using the long-run real-time PCR-based method (LORD-Q). Semi-long amplicons of around 1.5–2 kb can also enhanced sensitivity for detecting DNA damage (Zhu and Coffman, 2017).

2. Material & methods

2.1. Sampling and sample preparation

The wastewater effluent was collected biweekly from the local WWTP on the Karlsruhe Institute of Technology (KIT) campus in Karlsruhe Germany. It primarily consisted of wastewater from scientific research institutes, serving approximately 3300 individuals, including international scientists and students present during the week. The WWTP processes approximately 450 m^3 wastewater daily through a combination of conventional physical-chemical and biological treatment methods, including adsorption, precipitation, flocculation, and oxidation. Some chemical and physical average data collected are presented in Table S1. The treated WWTP effluent is discharged into the River Rhine.

Due to its unique composition, WWTP effluent required comprehensive analysis, as wastewater from scientific institutes can pose potential risks to the environment. For each aBL treatment (i.e., (i) aBL alone, (ii) aBL combined with TMPyP, and (iii) aBL combined with H_2O_2) at each of the three wavelengths 405 nm, 420 nm, 460 nm, respectively, nine samples were collected from the WWTP, resulting in nine sampling campaigns per trial. The study was conducted over three independent trials ($n = 3$). 4 L of effluent was collected from the WWTP at each campaign. For each aBL treatment, a minimum of three independent trials were conducted to ensure the reliability and reproducibility of the results. The collected wastewater was pumped into the photoreactor (Fig. 1; Figure S2) using a peristaltic pump (1 L min^{-1}). The wastewater samples underwent a circulation of 4 h within the aBL reactor, resulting in an absolute aBL irradiation of 26 min by the LED lamp passing the photo-chamber. An aliquot of 0.7 L of aBL-treated samples were taken at regular intervals to assess the effectiveness of the aBL irradiation. Test were carried out at one of the three wavelengths 405 nm, 420 nm, or 460 nm, respectively. We further investigated the shading effects caused by the particulate matter contained in the WWTP treated effluent. In theory particles may block aBL irradiation, creating areas without exposed to the rays, and then reducing the effectiveness of ROS production as microorganisms in these shadowed areas may not exposed to the aBL and therefore may not be inactivated. However, a relatively low suspended solids content of <0.1 mg L^{-1} measured in the KIT WWTP treated effluent implies that this shading effect on our aBL irradiation tests was marginal or absent.

The aBL treated water samples were subsequently stored in darkness at room temperature to inhibit any additional photoreactive transformations. Aliquots of 150 mL from each sample were filtered through polycarbonate membranes (PC) with 47 mm diameter and 0.2 μm pore size (Whatman Nucleopore Track-Etched Membranes, Sigma-Aldrich, Munich, Germany). Following filtration, the membranes were treated with 20 μM of propidium monoazide (PMA) for differentiating living from dead bacteria. PMA is able to enter the bacterial cell reaching the chromosomal and extrachromosomal nucleic acid due to the loss of cellular membrane integrity of injured/dead bacteria (Nocker et al., 2018; Cong et al., 2023). This modified DNA is blocked for subsequent qPCR analyses. The procedure was completed by incubating the PMA-treated and filtered biomass in a dark environment for 10 min to prevent any photodegradation of the PMA. Then the filtered biomass on membranes were exposed to the PhAST Blue Photo-Activation System (GenIUL, Barcelona, Spain) at maximum intensity for a duration of 15 min for cross-linking of PMA with the DNA of the dead/injured bacterial cells.

2.2. Continuous flow aBL photoreactor

The continuous flow photoreactor, as described below, is initially designed as a laboratory system to test its inactivation efficiency. Decentralized use with up-scaling is planned for subsequent studies once the appropriate operating parameters have been determined.

The continuous flow aBL reactor experimental setup used for wastewater irradiation comprised of a sample tank, a peristaltic pump, a reactor cabinet (including one LED lamp with one wavelength), and a LED power supply. Additionally, a waste container was utilized for storing the treated wastewater, while 70 % isopropanol was employed for disinfecting the setup (Fig. 1). The aBL photoreaction chamber featured a dual glass cylinder setup, comprising an outer and an inner glass cylinder. Into the inner glass, a LED lamp was inserted centrally, whereby the flow of the test water was circulated upwards around the LED lamp. A peristaltic pump for transferring wastewater from the sample reservoir to the reactor cabinet, an LED cooling device to regulate system temperature, and a power supply for adjusting LED intensity.

Fig. 2 shows the calculated duration time of irradiation in the LED based reaction chamber's area (highlighted in blue), which spans 26 s by a given flow rate of 1 L min^{-1} dictated by the pump. The total volume of the chamber subjected to irradiation was 0.43 L. Within the inner cylinder, a LED mounting base equipped with four surfaces accommodates the LEDs. This base was hosted 12 LEDs arrayed in a row on each of its surfaces. The LED configuration delivered specific light intensities for aBL treatments at various wavelengths, where 420, 405, and 460 nm

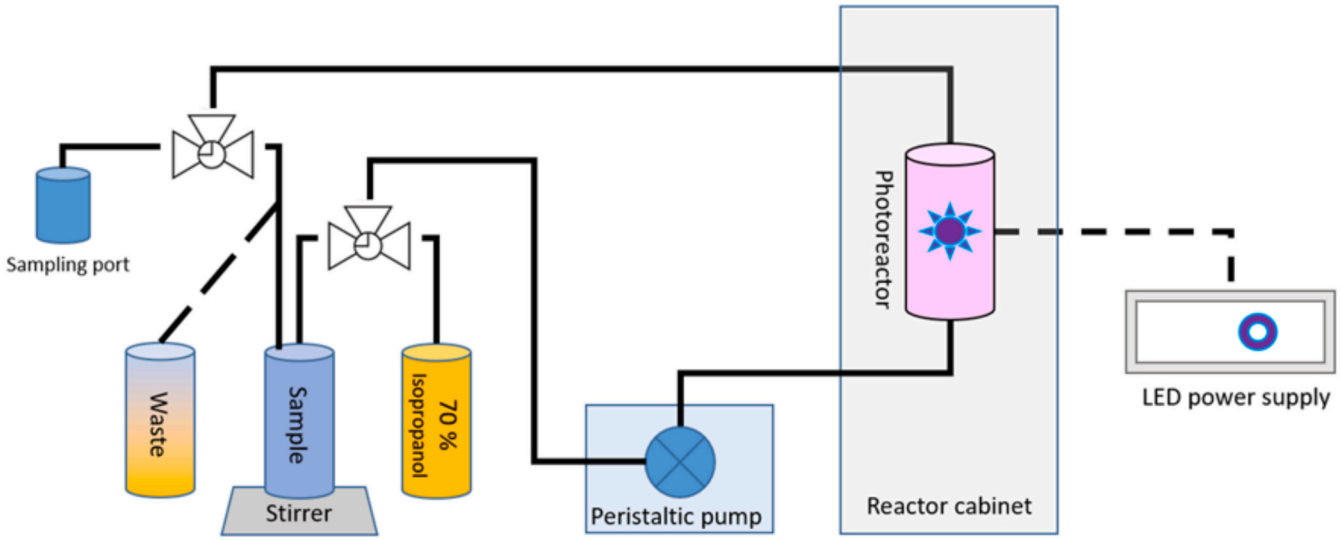

Fig. 1. The experimental setup used in the water irradiation process using a continuous flow aBL photoreactor.

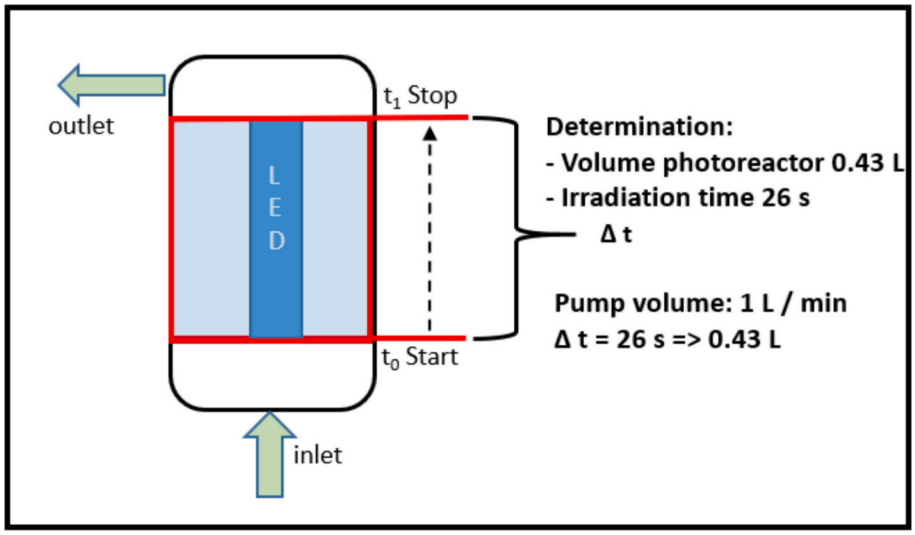

Fig. 2. The schematic diagram of the reactor illustrates a total volume of 0.43 L and a retention of irradiation time of (Δt = t1-t0) 26 s for the wastewater passing through the LED-irradiated volume at a flow rate of 1 L min^{-1}.

achieved 2758, 3282, and 3486 W m^{-2}, respectively. The time dependent energy input corresponds with 430 J cm^{-2} at 420 nm, 512 J cm^{-2} at 405 nm, and 544 J cm^{-2} at 460 nm for 26 min. The energy input for 13 min irradiation was calculated with 215 J cm^{-2} at 420 nm, 256 J cm^{-2} at 405 nm, and 272 J cm^{-2} at 460 nm. Finally, the energy input for 6.5 min irradiation was 108 J cm^{-2} at 420 nm, 128 J cm^{-2} at 405 nm, and 136 J cm^{-2} at 460 nm. Based on a specified volume of 4 L of WWTP effluent being fed into the photoreactor without any pretreatment, the calculated entire irradiation time of the total volume of water sample in the photo reactor chamber for the residence time of (Δt = t1-t0) 26 min at a flow rate of 1 L min^{-1} for 4 h. The time points T0, T1, T2, and T4, corresponded to the untreated sample, one-hour treatment, two-hour treatment, and four-hour treatment, respectively, thus reflecting operation times. However, the total irradiation times differed with 6.5 min for T1, 13 min for T2, and 26 min for T4.

2.3. DNA extraction for molecular biological analyses

DNA was extracted using the FastDNA™ Spin Kit for Soil (MP Biomedicals, Santa Ana, USA) and the FASTPREP® device (MP Biomedicals, Santa Ana, USA). For mechanical cell disruption, the filtered biomass on membranes were placed in the Lysing Matrix E tube and treated according to the manufacturer's protocol. Proteins were separated by centrifugation and precipitation, and the DNA was finally purified by attachment to a silica matrix. The concentration of extracted DNA was measured using the NanoDrop (ND-1000, PEQLAB Biotechnologie GmbH, Germany) and the Quant-iTTM PicoGreen® dsDNA Assay Kit (Thermo Fisher Scientific, Nidderau, Germany).

2.4. Quantitative PCR (qPCR) analysis

SYBR Green qPCR assays were performed using a Bio-Rad Cycle CFX96 (CFX96 TouchTM Deep Well Real-Time PCR Detection System, Bio-Rad, Munich, Germany), and analysis was performed using the manufacturer's software (Bio-Rad CFX Manager Software). Reactions were performed in volumes of 20 μL containing 10 μL Maxima SYBR Green/ROX qPCR Master Mix (2×) (Thermo Scientific Nidderau, Germany), 7.4 μL nuclease-free water (Ambion, Life technologies, Karlsbad, Germany), 0.8 μL primer forward (10 μM), 0.8 μL primer reverse (10 μM) and 1 μL template DNA. In the denaturation phase, double-stranded DNA was converted into single strands by heating at a high temperature (about 95 °C) for 10 min. This was followed by 40 cycles of 15 s at 95 °C and 60 s at 60 °C. The melting curves were recorded by increasing the temperature from 60 °C to 95 °C (1 °C every 10 s) to assess the specificity of the application. The clinical relevance of the investigated ARGs and FPB are shown in Table 1. For each target (ARGs or FPB), the primer sequences used are listed in Table S2. Information on the characteristics and quality of the qPCR systems used for the taxonomic genes and the antibiotic resistance genes is given in Table S2. Cq (quantification of cycle) stands for cycle threshold and refers to the number of times a machine must copy a piece of genetic material before it can be detected in a PCR test. The value represents the amount of genetic material in a particular sample at a specific point in time. In general, the lower the Cq value, the higher the load that is found in the sample, while the higher the Cq value, the lower the load is. previous experience (Hembach et al., 2019, 2022; Cong et al., 2023). The different ARG clusters categorize ARGs into common, moderate and rare gene targets and are based on previous experience (Hembach et al., 2019, 2022; Cong et al., 2023).

Table 1
Categorization of various FPB and ARGs is based on their abundance, stated as median of cell equivalents per 100 mL (n = 3), within the KIT WWTP.

	Targets	Median of cell equivalents per 100 mL	Median absolute deviation (MAD)
Eubacteria	16S rDNA	6.39E+08	1.72E+08
Facultative pathogenic bacteria (ESKAPE group)	*yccT (E. coli)*	4.18E+05	1.62E+05
	23S *(enterococci)*	4.18E+03	1.82E+03
	secE (A. baumannii)	2.02E+02	5.38E+00
	ecfX (P. aeruginosa)	9.34E+01	2.24E+01
Commonly detected	*sul*1	3.54E+07	4.56E+06
	*Intl*1	1.79E+06	4.02E+05
	*tet*M	1.45E+05	6.49E+04
	*erm*B	1.26E+05	1.88E+04
	bla_{TEM}	8.40E+04	2.06E+04
Intermediately detected	bla_{VIM}	3.67E+03	1.41E+03
	$bla_{CTX-M32}$	2.58E+03	1.51E+03
	bla_{OXA-48}	6.87E+02	5.44E+02
	bla_{CTX-M}	3.32E+02	2.12E+02
	bla_{CMY-2}	2.35E+02	8.33E+01
	mcr-1	8.56E+01	5.85E+01

2.5. The photosensitizer porphyrin TMPyP and the oxidative agent H_2O_2

The photosensitizer porphyrin TMPyP (5,10,15,20-Tetrakis-(*N*-methyl-4-pyridyl)21,23-porphyrintetratosylate) was obtained from Sigma-Aldrich in Darmstadt, Germany, and its structure is depicted in (Figure S1). The 1×10^{-3} M TMPyP stock solution was preserved at a storage temperature of 4 °C. For experimental purposes, a higher dilution, 1×10^{-6} M, was added to the water samples. The concentrations used for TMPyP are based on studies that have proven to be particularly effective in reducing antibiotic resistance (Cong et al., 2023). The molecular structure of TMPyP is characterized by a planar, tetracationic structure, centered around a porphyrin ring enabling porphyrin molecules to absorb light across a specific spectrum and making them effective in photodynamic applications. Additionally, 1 mM H_2O_2 was added to the water samples to explore the inactivation potential for ARG and FPB during aBL treatment.

1 mM H_2O_2 was used which is correlated with the optimal concentration used in the study (Truong et al., 2020). The higher concentration of H_2O_2 can cause scavenging of $HO^{\bullet}$ by H_2O_2. In principle, it has been shown that both TMPyP (1×10^{-6} M) and H_2O_2 (1 mM) has no antibacterial effects without blue light irradiation (data not shown). Only irradiation with blue light of the specified wavelengths showed an additional antibacterial capacity by the two components.

2.6. Cultivation of facultative pathogenic bacteria

Before (untreated wastewater) and after (treated wastewater) aBL irradiation, 50 mL of each sample were filtered through a nitrocellulose membrane (0.45 μm, GE Healthcare Life Sciences, Solingen, Germany) in preparation for cultivation. Selective agar plates were assessed by cultivation for the efficiency of aBL treatment. Four different agar plates were used in this investigation: CHROMagar™ ESBL, Enterococci agar plates, Pseudomonas agar plates, and CHROMagar™ Acinetobacter. CHROMagar™ ESBL allows enrichment of extended-spectrum beta-lactamases (ESBLs) producing bacteria), enzymes confer resistance to a wide range of beta-lactam antibiotics, including penicillins and cephalosporins. Enterococci agar plates are used for the selective isolation and identification of *Enterococcus* species from clinical and environmental samples. Pseudomonas agar plates are used for the selective isolation and identification of *Pseudomonas* species, particularly *Pseudomonas aeruginosa*, from clinical and environmental samples. CHROMagar™ Acinetobacter are used to selectively isolate and identify *Acinetobacter* species. The Colony Forming Units (CFU) were quantified for 50 mL water sample volumes after overnight incubation. The fold change in bacterial count was calculated by taking the ratio of the bacterial count after treatment (C_t) to the initial bacterial count (C_0), expressed as C_t/C_0. A fold change of 1 means no change, >1 indicates an increase, and <1 indicates a decrease.

2.7. DNA damage analysis by qPCR

The methodology involves amplifying genomic DNA extracted from aBL-irradiated samples (aBL treatment alone, aBL treatment with TMPyP, and aBL treatment with H_2O_2) using "short" and "long" qPCR reactions. We used with approximately 1500 bp long amplicons to balance sensitivity and efficiency in quantifying DNA damage. The resulting Cq values and the amplification efficiencies of the two reactions are calculated using the eq. E = [10(−1/slope)-1]. Correlation coefficients (R2) are derived from standard curves generated by running qPCR reactions on serial dilutions of the samples. In the investigation of DNA damage, a diverse array of primer types, as specified in Table S2, was utilized. The primer 27F, referred to as primer F_L, and BacUni-1387F, referred to as primer F_S, were each paired with the identical reverse primer BacUni-1492R, identified as primer R. This configuration facilitated the generation of both long and short amplicons. All qPCR reactions were executed in volumes of 20 μL, consistent with the established protocol for detecting target sequences through qPCR. For the elongation of sequences with approximately 1500 base pairs in length, the cycling protocol commenced with a three-minute polymerase activation phase at 95 °C, followed by 39 cycles of 15 s at 95 °C, 20 s at 55 °C, and 80 s at 72 °C. Conversely, the amplification of shorter (approximately 100 base pairs) sequences, adhered to a similar initial step of three minutes at 95 °C for polymerase activation, but was followed by 39 cycles of 15 s at 95 °C, 20 s at 55 °C, and 15 s at 72 °C. The Cq values was automated via the Bio-Rad CFX Manager software, and the subsequent data analysis was conducted using Microsoft Excel. This method ensured precise and repeatable measurement of DNA amplification across varying experimental conditions. To quantify DNA lesions per 10 kb, the Cq values correlate to the number of target copies obtained from the experiments. Together with the amplification efficiencies of the two reactions and the amplicon lengths, were processed using the LORD-Q equation (Dannenmann et al., 2017).

2.8. Statistics

For statistical evaluation, the median cell equivalent from all sample collection campaigns was used to calculate *p*-values for the significance displayed in our figures. The statistical significance of the experimental data was rigorously evaluated using Analysis of Variance (ANOVA) tests, followed by Tukey's multiple comparisons analysis. The comparisons were made between the control group, aBL treatment alone, and aBL treatment in conjunction with either TMPyP or H_2O_2. The outcomes of these analyses are reported as follows: non-significant (ns), $^{*}P \leq 0.5$, $^{**}P \leq 0.05$, $^{***}P \leq 0.01$. The median abundance of WWTP effluent was calculated by averaging the cell equivalents obtained from three sample trials. The Median Absolute Deviation (MAD) represents the statistical dispersion, and was calculated as.

$$XY = (|x_i - \text{median}(x_i)|),$$

where x_i represents the cell equivalents of each individual data point in the dataset, and i denotes the index corresponding to each specific data point.

3. Results and discussion

3.1. Reduction effectiveness of FPB in the aBL photoreactor determined by cultivation

The presence of FPB and ESBL producing bacteria was elucidated by culturing. Specifically, the Gram-positive bacteria *Enterococcus* spp. and Gram-negative *Acinetobacter* spp. and *Pseudomonas* spp. were selected for cultivation on selective media from untreated and treated wastewater samples with blue light and in combination with TMPyP or H_2O_2. Additionally, bacteria producing extended spectrum of beta-lactamases from the ESKAPE group were studied by cultivating experiments. The initial colony-forming units (CFUs) for *Enterococcus* spp., *Acinetobacter* spp., and ESBL agar plates were determined to be 1326 ± 75, 837 ± 43, and 390 ± 82 CFUs per 100 mL, respectively. These values represent the mean results and standard deviations obtained from three independent trials.

As shown in Fig. 3, a progressive reduction in CFU counts was observed from 0 h (no treatment) to 4 h (i.e. 26 min real aBL irradiation). This was observed for 405, 420, and 460 nm of aBL treatment, as well as in presence of TMPyP or H_2O_2 together with aBL irradiation. This trend was observed across all tested FPB, irrespective of the wavelengths applied. When evaluating the susceptibilities of these bacterial species, *Enterococcus* spp. (Fig. 3a) exhibited higher sensitivity to aBL treatment than *Acinetobacter* spp., *Pseudomonas* spp., and ESBL-producing bacteria. One-hour aBL irradiation, regardless of the wavelength, completely inhibited the growth of this Gram-positive bacterium *Enterococcus* spp., indicating complete inactivation by aBL alone and when combined with

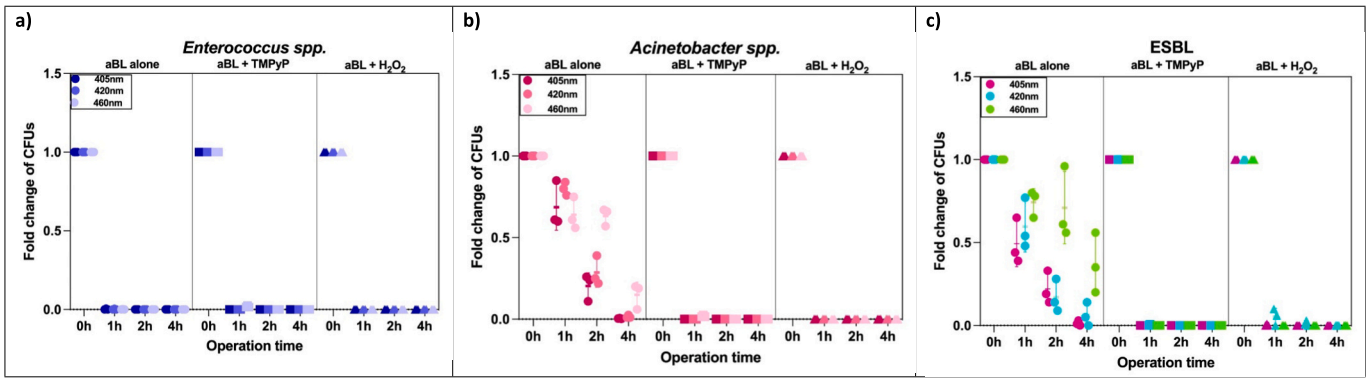

Fig. 3. The fold change of CFU from subsequent (Ct) to initial (C0) concentration values at four time points (0 h, 1 h, 2 h, 4 h) following nine different aBL treatments, including aBL alone, aBL combined with H_2O_2, and aBL combined with TMPyP at three distinct wavelengths. In total, nine sampling campains were done. Each dot represents the results of an individual trial for each wastewater treatment condition ($n = 3$).

TMPyP or H_2O_2 (Fig. 3a). This increased sensitivity may be due to the absence of the specific outer membrane in Gram-negative bacteria, making them more resistant to oxidative stress than Gram-positive bacteria (Maldonado-Carmona et al., 2022). For *Acinetobacter* spp. (Fig. 3b) as well as for ESBL producing bacteria (Fig. 3c), the combination of aBL with TMPyP or H_2O_2 demonstrated superior effectiveness in CFU reduction compared to aBL treatment alone, as evidenced by the complete absence of colonies on the specific agar plates after 4 h irradiation. Nevertheless, it became evident that the effectiveness of aBL treatment is dynamic and influenced by multiple factors beyond just wavelength (e.g. Gram positive vs Gram-negative). However, its impact on inactivating FPB becomes increasingly evident over time. *Pseudomonas* spp. count numbers were too high to quantify in all untreated wastewater samples, making fold change calculation impossible. However, aBL irradiation reduced CFUs. Compared to other pathogens, *Pseudomonas* spp. were less sensitivity to the treatment highlighting their high resilience compared to the other FPBs. In conclusion, aBL treatment combined with TMPyP or H_2O_2 enhanced the reduction of FPB and ESBL bacteria. Comparing the CFU reduction data 405 and 420 nm were slightly more effective compared to 460 nm after 1 h of treatment. These differences disappeared in case of longer treatment times. This may be due to the higher photon energy of 405 nm and 420 nm aBL compared to 460 nm at the beginning of the treatment, when all intracellular involved structures are more or less intact (Enwemeka et al., 2021; Huang et al., 2023), which induces more ROS and increases oxidative stress potentially leading to more viable but non-culturable (VBNC) states in bacteria. It was shown, that >100 bacterial species have been found to enter a VBNC state under oxidative stress conditions (Ayrapetyan et al., 2018). Additionally, bacteria that are unable to withstand multiple stressors have also been shown to transition into the VBNC state (Idil et al., 2011; Barber, 2015). Hence, the VBNC state need to be analysed by living/dead staining in planed subsequent studies. It should be noted that cultivation experiments may be biased due to the limitations of cultivation methods in general. Therefore, incorporating molecular biology techniques was crucial to accurately assess bacterial viability and response to aBL treatments.

3.2. Reduction effectiveness of FPB and ARB during aBL irradiation as determined by qPCR

3.2.1. FPB and ARGs abundances in WWTP effluent

The total bacterial load in the WWTP effluent, quantified via the eubacterial ribosomal 16S rDNA using qPCR, averaged 6.39×10^8 cell equivalents per 100 mL (Table 1). The *intI1* gene, coding for a transposon-based Class I integrase, serves as a specific marker for class 1 integrons and indicates the potential for HGT, was present at 1.79×10^6 gene copies per 100 mL. An increased gene transfer rate facilitated by the dissemination of *intI1*, may facilitate to its spread through the corresponding gene cassettes in mobile genetic elements.

Lower abundances for specific taxonomic gene markers were detected for the FPB of the ESKAPE group (Table 1): Detected species included enterococci (23S rDNA gene), *Pseudomonas aeruginosa* (*ecf*X gene), *Acinetobacter baumannii* (*sec*E gene), and *Escherichia coli* (*ycc*T gene) (Table 1). *E. coli,* detected using the *ycc*T was the dominant species with an average of 4.18×10^5 cell equivalents per 100 mL. *E. coli,* serving as a well-known indicator for fecal contaminations. *Enterococci* was also abundant, with 4.18×10^3 cell equivalents per 100 mL. *P. aeruginosa* and *A. baumannii* were detected in lower concentrations, with 1–2 logs per 100 mL. The abundance of ARGs was categorized into 'commonly detected genes' and 'intermediately detected genes' based on previous studies (Hembach et al., 2019) (Table 1). 'Commonly detected genes' include *erm*B (resistance to erytrhomicin in Gram positive bacteria like *Enterococcus*, *Staphylococcus*, and *Streptococcus*), *sul*1 (resistance to sulfonamides, often found in mobile genetic elements, such as plasmids, transposons, and integrons), *tet*M (tetracycline resistance, frequently detected in wastewater from hospitals, agricultural runoff, and residential areas), and $bla_{\mathbf{TEM}}$ (a beta-lactam resistance gene, commonly detected ESBL gene) (Wang et al., 2022; Gao et al., 2012; Wen et al., 2016; Sah and Hemalatha, 2015). These genes exhibited cell equivalent concentrations ranging from 10^4 to 10^7 log units per 100 mL in the WWTP effluent making them suitable for assessing ARG inactivation effectiveness in wastewater treatment. 'Intermediately detected genes' include $bla_{\text{CTX-M}}$, $bla_{\text{CTX-M32}}$, $bla_{\text{OXA-48}}$, $bla_{\text{CMY-2}}$, and bla_{VIM}, which are beta-lactam resistance genes associated with FPB with two and three log level abundances. The colistin resistance gene *mcr-1,* carried by *Enterobacteriaceae* on transmissible plasmids, has previously been reported in municipal and husbandry WWTPs (Savin et al., 2021). We found *mcr-1* at low abundance, indicating its presence but at lower concentrations compared to other ARGs. Other critical ARGs, including *van*A, bla_{NDM}, and *mec*A were not detected in the WWTP effluent.

Our results imply high contamination of FPB from the ESKAPE group in WWTP effluent. ESKAPE group pathogens, among other health-concerning microorganisms of, are clinically important bacteria responsible for many community and hospital-acquired infections (Mathur et al., 2023). Even without direct inputs from clinical facilities, industry, or agriculture, critical facultative pathogenic bacteria (Table 1, Fig. 3) enter local wastewater, persist through and remain unaffected by most conventional treatment processes, and ultimately reach receiving water bodies. Our study suggests that the international community at the KIT campus contributes to the dissemination of a broad spectrum of ARGs and FPB to the KIT WWTP due to the incomplete effectiveness of the current wastewater treatment processes. Therefore, it is essential to consider implementing a supplementary quaternary treatment step for hygienization with advanced wastewater treatment methods, such as

aBL-photo disinfection, and to evaluates its effectiveness.

3.2.2. Effectiveness of aBL irradiation at different wavelength to inactivate FPB and ARG

The effectiveness of three aBL wavelengths in inactivating FPB and ARG in KIT WWTP effluent was evaluated (Table S3). Among the detected FPB, enterococci demonstrated sensitivity to all three aBL wavelengths. Notably, treatment with 420 nm aBL achieved a maximum reduction of 2.6 $\log_{10}$ units (Fig. 4a). Although the 405 nm aBL wavelength resulted in a comparatively lower reduction of enterococci, the bacteria remained susceptible to aBL treatment alone. This finding is further corroborated by results obtained through cultivation-based methods. For other Gram-negative bacteria, aBL treatment alone appears insufficient for effective inactivation (Fig. 4a). *P. aeruginosa* exhibited a higher tolerance to aBL, showing no significant reduction in gene copy numbers after 4 h of exposure, regardless of the wavelength. This observation aligns with the cultivation-based results, further confirming the bacteria resistance to aBL treatment alone. When using aBL treatment alone for bacterial inactivation, the specific wavelength of aBL does not appear to be a critical factor in the removal of FPB. Instead, the intrinsic characteristics of the bacteria themselves may play a more significant role in determining their susceptibility to aBL treatment (i.e., Gram-positive vs Gram-negative bacteria). The incomplete disinfection may be due to insufficient irradiation during the 4-h flow reactor experiment, which did not achieve high enough intracellular ROS concentrations to inactivate targeted FPB/ARGs.

Among the examined ARGs, the susceptibility to aBL treatment varied which might depend on the bacterial host carrying the gene under investigation. Frequently detected ARGs, such as *erm*B, which encodes resistance to erythromycin, exhibited the strongest reduction, reaching up to 1.9 $\log_{10}$ units following irradiation with 420 nm aBL (Fig. 4b). Similarly, the *tet*M gene, responsible for tetracycline resistance, displayed moderate susceptibility to aBL treatment, with a reduction of up to 1.8 $\log_{10}$ units at 420 nm (Fig. 4b). Other intermediately detected ARG targets, including $bla_{\text{CTX-M}}$, $bla_{\text{CTX-M32}}$, $bla_{\text{CMY-2}}$ were less efficiently inactivated by aBL irradiation. The bla_{VIM} and *mcr*-1 genes exhibited relatively high sensitivity to aBL treatment alone, with reductions in gene copy numbers of 1.9 $\log_{10}$ and 0.9 $\log_{10}$, units respectively, following irradiation with 420 nm aBL (Fig. 4c). When aBL was applied alone, the extent of ARG reduction appeared to be highly dependent on the specific bacterial hosts carrying the genes as part of the real wastewater effluent. Furthermore, the additional wavelengths of aBL (405 nm and 460 nm) did not appear to have a significant or decisive impact on ARG reduction.

There are clear differences in the results (1) when comparing culture methods with qPCR, and (2) when comparing the flow-through reactor with the static aBL photosystem reported by Cong et al. (2023). In the culture method, FPB contamination in the wastewater was reduced to 0 CFU after 4 h aBL irradiation (26 min, without addition of photosensitizers or oxidative agents) (Fig. 3). However, qPCR analysis showed a less acceptable reduction. This discrepancy could be due to sufficient cellular DNA still being available for qPCR, despite the bacterial cells losing cultivability due to aBL treatment. Possible reasons include shading effects, bacterial aggregating, insufficient DNA degradation by ROS, and matrix effects impacting PMA treatment for living/dead discrimination. Irradiation exceeding 4 h and a simultaneous application of 405 nm, 420 nm, and 460 nm wavelengths are recommended for future applications of the aBL method to achieve higher inactivation. Cong et al. (2023) showed that simultaneous irradiation of wastewater from slaughterhouses with the three wavelengths of blue light in the static photoreactor resulted in strong reductions up to elimination within 4 h; with the photosensitizers significantly increasing reduction performance. The energy input in J cm^{-2} was generally 10 times higher in the static aBL photosystem compared with the recently used flow through photoreactor (Cong et al., 2023).

Consistent with the results for taxonomic gene markers, the calculated ARGs reduction rates (Fig. 4b and c) imply that no full inactivation was achieved by aBL at the maximum irradiation of 26 min (equal to 4 h of operation). This demonstrates that aBL irradiation could inactivate FPB and ARGs to a certain extent within the applied treatment period, independent of the wavelength, although effectiveness was likely limited by insufficient internal ROS production. Matrix effects of the wastewater, aggregate formation (hindering light penetration), and shading effects are plausible explanations for the limitation of aBL irradiation. Therefore, the application of effective additional photosensitizers is crucial for enhancing the efficiency of aBL treatment, particularly in overcoming the limitations of aBL alone in inactivating certain FPB and ARGs.

3.2.3. Comparative effectiveness of added TMPyP or H_2O_2

TMPyP, a photoactive dye, has been shown to inactivate microorganisms in combination with aBL irradiation very efficiently (Cong et al., 2023). Porphyrins are organic chemical structures with four pyrrole rings, connected by four methine groups, forming cyclic structures and are present in different bacterial cytochromes (Fig. S1). The integration of blue light therapy with exogenously applied oxidizing agents like hydrogen peroxide (H_2O_2), has been adopted in medical photodynamic therapies (Ngo et al., 2023). H_2O_2 enhances the efficiency of light-induced processes, such as UV-C, in eliminating pollutants by generating free radicals (HO• or/and SO_4 •-) (Guan et al., 2020).

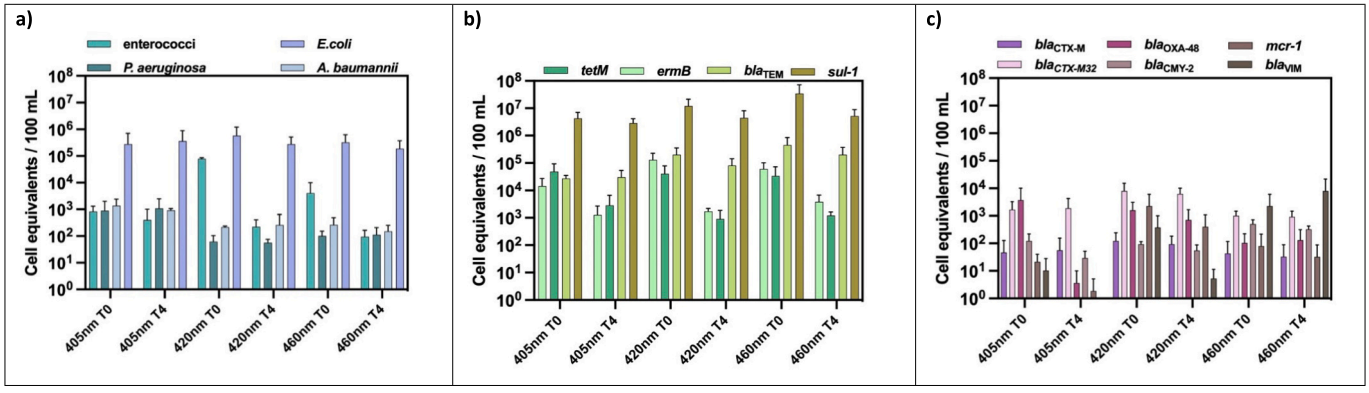

Fig. 4. FPB and ARG cell equivalents per 100 mL in untreated wastewater effluent samples (T0) and wastewater samples treated with aBL alone at 405, 420, and 460 nm after 4 h (T4) reactor operation (equal to 26 min net irradiation). The results are categorized into three groups: (a) FPB, including *enterococci*, *Pseudomonas aeruginosa*, *Acinetobacter baumannii*, and *Escherichia coli*, (b) commonly detected ARGs, including genes such as *ermB*, *tetM*, bla_{TEM}, and *sul1*, (c) intermediately detected ARGs, including $bla_{\text{CTX-M}}$, $bla_{\text{CTX-M32}}$, $bla_{\text{OXA-48}}$, $bla_{\text{CMY-2}}$, *mcr-1*, and bla_{VIM}. Values are averages from n = 3 tests at each condition, and the bars represent the standard deviation of the triplicates.

While aBL is effective in removing FPB, its successful application in eliminating ARB/ARGs from wastewaters has not been thoroughly investigated. The usefulness of aBL irradiance alone and in combination with TMPyP and H_2O_2 in inactivating selected FPB and ARG targets in WWTP effluents was investigated (Table S4). Fig. 5 shows the effectiveness of three different aBL treatments, expressed as cell equivalence per 100 mL for selected gene targets categorized into four groups, with (a) 16S rRNA gene and *intI1*; (b) FPB, including enterococci, *P. aeruginosa*, *A. baumannii*, and *E. coli*; (c) Commonly detected ARGs, including *erm*B, *tet*M, bla_{TEM}, and *sul*1; (d) Intermediately detected ARGs, including $bla_{CTX\text{-}M}$, $bla_{CTX\text{-}M32}$, $bla_{OXA\text{-}48}$, $bla_{CMY\text{-}2}$, *mcr-1*, and bla_{VIM}. As 420 nm proved to be quite similar effective among the three tested wavelengths, we focused on it.

In our study, an antibacterial effect of added H_2O_2 (1 mM) is only seen in combination with aBL irradiation (data not shown). Hydrogen peroxide itself does not absorb light strongly in the visible spectrum or in the spectral range of the emitted blue light. But when combined with certain catalysts or photosensitizers (like titanium dioxide, silver nanoparticles, or certain organic compounds like photoenhancers or intracellular light sensitive compounds), the system can absorb light in the blue range (400–460 nm).

Photosensitizers which absorb blue light enter an excited state, either a singlet or a triplet excited state, depending on the nature of the sensitizer. In its excited state, the photosensitizer can interact with hydrogen peroxide molecules. This interaction can lead to the enhanced production of reactive oxygen species (ROS), such as hydroxyl radicals (•OH) and singlet oxygen ($^1O_2$). In summary, the activation of hydrogen peroxide under blue light involves the absorption of light by a photosensitizer, which then produces reactive oxygen species that decompose H_2O_2. The presence of blue light and a suitable catalyst is critical to this process. Further, although H_2O_2 is described as a toxic molecule and also occurs naturally as part of the bacterial energy metabolism, it is naturally degraded or intercepted by scavenger molecule activities like porphyrins and can then no longer show its bactericidal potential. However, if these intracellular scavenger molecules are altered by aBL irradiation, their scavenger potential is lost and the antibacterial potential of H_2O_2 comes into play. The different behaviour of bacteria in natural communities or reference bacteria can therefore be attributed to different intracellular concentrations of natural scavenger molecules or their enzymatic activities (Mishra and Imlay, 2012; Yoon et al., 2022).

It must be noted that the added photosensitizer TMPyP (10^{-6} M) and the oxidative agent H_2O_2 (1 mM) showed no reducing effect on bacterial

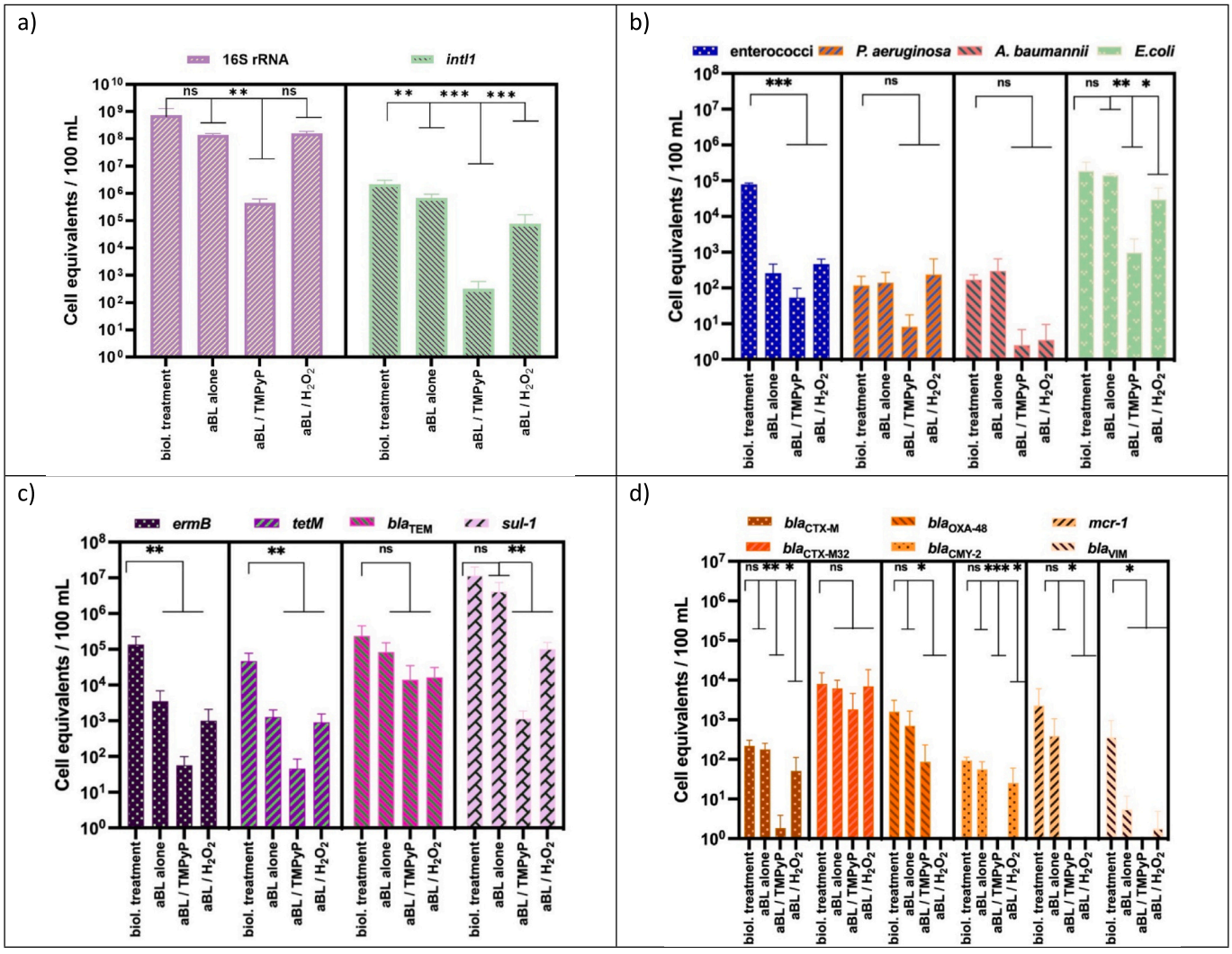

Fig. 5. Cell equivalents per 100 mL of FPB and ARGs at aBL irradiation for 4 h (equal to 26 min irradiation) using aBL alone at 420 nm, aBL + TMPyP (10^{-6} M), and aBL + H_2O_2 (1 mM). Results are categorized into four groups: (a) 16S rRNA and *intI1*, (b) FPB, including *enterococci*, *Pseudomonas aeruginosa*, *Acinetobacter baumannii*, and *Escherichia coli*, (c) commonly detected ARGs, including *ermB*, *tetM*, bla_{TEM}, and *sul1*, (d) intermediately detected ARGs, including $bla_{CTX\text{-}M}$, $bla_{CTX\text{-}M32}$, $bla_{OXA\text{-}48}$, $bla_{CMY\text{-}2}$, *mcr-1*, and bla_{VIM}. Values are average from n = 3 tests at each condition. The statistical significance of the differences in treatment effects is indicated by asterisks.

communities without aBL irradiation. Only with simultaneous aBL irradiation did the additional reduction performance of aBL develop in wastewater effluent (data not shown, but available upon request). The combination of aBL with TMPyP significantly decreased 16S rRNA gene abundance, indicating a strong bactericidal effect and reduced overall bacterial load (Fig. 5a). In contrast, aBL alone and its combination with H_2O_2 did not significantly reduce 16S rRNA genes, suggesting these treatments were less effective at lowering bacterial load. Regarding the *intl1* gene, Fig. 5a shows varying levels of effectiveness among the three treatments: aBL alone led to a reduction of <1 $\log_{10}$ in *intl*1 gene copies, indicating a modest impact on the HGT marker. The combination of aBL with H_2O_2 resulted in greater reduction, achieving a 1.4 $\log_{10}$ decrease. aBL combined with TMPyP achieved the strongest reduction, reaching up to approximately 4 $\log_{10}$ units, highlighting TMPyP's significant role in enhancing aBL's ability to target and reduce ARGs, particularly those associated with integrons like *intl1*. This implies that the combination of aBL with TMPyP exhibits enhanced ability to inactivate ARGs compared to H_2O_2. aBL irradiation alone led to a significant reduction in gene copy numbers, specifically a 2.5 $\log_{10}$ decrease observed in enterococci (Fig. 5b). In contrast, gene copy numbers of *P. aeruginosa*, *A. baumannii*, and *E. coli* remained unchanged, even after 4 h of aBL irradiation (equal to 26 min of aBL net irradiation). This discrepancy highlights the varying susceptibility of different FPB to aBL irradiation, confirmed by our cultivation methods. The combination of aBL with TMPyP resulted ina 3.3 $\log_{10}$ reduction for enterococci, 1.2 $\log_{10}$ for *P. aeruginosa*, 1.8 $\log_{10}$ for *A. baumannii*, and 2.4 $\log_{10}$ for *E coli (*Fig. 5b). This demonstrated that combining TMPyP with violet-blue light significantly enhanced the reduction of multidrug-resistant strains of *P. aeruginosa* and *Klebsiella pneumoniae,* supporting previous studies such as by Mušković et al. (2023). However, adding H_2O_2 appears more selective strongly inactivating *A. baumannii*, a bacterium known for its resistance mechanisms, but not enhancing the inactivation of enterococci, *P. aeruginosa*, and *E. coli* beyond what was achieved with aBL with TMPyP.

Based on the results of each specific target gene (Table 1, Fig. 5), ARGs n the KIT WWTP effluent can be categorized into two groups. The first group includes commonly detected ARGs, such as *erm*B and *tet*M genes, which are more susceptible to aBL irradiation (Fig. 5c). These genes were reduced of approximately 1.5 orders of magnitude with aBL alone. Adding H_2O_2 at 1 mM enhanced effectiveness by 2 orders of magnitude. Notably, combining TMPyP with aBL irradiation increased reduction effectiveness, resulting in a 3 $\log_{10}$ unit decrease. In contrast, the *sul*1 gene, less susceptible to aBL alone, was better inactivated with aBL and TMPyP, showing a 4.2 $\log_{10}$ unit decrease.

The combination of aBL with H_2O_2 also leads to a notable reduction, though less pronounced, with a decrease of 2.1 $\log_{10}$ units. The bla_{TEM} gene was more robust to all three aBL-treatments suggesting that bacteria with bla_{TEM} gene are less susceptible to the oxidative and photodynamic effects of aBL, whether used alone or in with TMPyP or H_2O_2. Regarding the second group (Table 1), the intermediately detected ARGs, including $bla_{CTX\text{-}M}$, $bla_{CTX\text{-}M32}$, $bla_{OXA\text{-}48}$, and $bla_{CMY\text{-}2}$, aBL irradiation alone did not substantially change gene copy concentrations, indicating minimal impact. However, the addition of TMPyP reduced $bla_{CTX\text{-}M}$ and $bla_{CMY\text{-}2}$ gene copy numbers by approximately 2 $\log_{10}$ units, suggesting that TMPyP significantly enhanced aBL irradiation effectiveness for these ARGs. In contrast, $bla_{CTX\text{-}M32}$ was more robust against aBL under similar conditions. Conversely, $bla_{OXA\text{-}48}$ was highly susceptible to aBL combined with H_2O_2, indicating that it can be effectively affected. The *mcr-1* gene was notably susceptible to both aBL with TMPyP and aBL with H_2O_2, demonstrating significant inactivation. This suggests that the combined oxidative and photodynamic effects are sufficient to significantly eliminate these gene or bacteria carrying them, which is crucial given the clinical importance of colistin resistance. On the other hand, bla_{VIM}, associated with carbapenem resistance, was unaffected by aBL treatment.

The maximum aBL irradiation time in this study was limited to 26 min, resulting from a total circulation time of 4 h for 4 l of WWTP effluent in the photoreactor. A longer circulation period or aBL irradiation time in combination with photosensitisers or H_2O_2 in an up-scaled variant is expected to result into a greater inactivation or elimination of FPB and ARGs. This was confirmed by experiments using a static aBL reactor with TMPyP as a photosensitizer, exhibiting much longer continuous irradiation durations in the range of several hours (Cong et al., 2023).

Conventional treatment processes at WWTPs often fail to completely eliminate ARB or ARGs, allowing them to enter downstream aquatic environments through effluent discharge (Alexander et al., 2020; Hembach et al., 2017). Implementing strategies to disrupt these transmission pathways and prevent selection processes can effectively mitigate the evolution and spread of antibiotic resistance. Identifying critical control points in sewer systems is crucial, with special attention to ARGs against reserve antibiotics, which are detected in intermediate or low abundances in wastewater systems via genetic detection methods (Uluseker et al., 2021; Alexander et al., 2022; Hembach et al., 2019).

As an outlook, after further optimization to real-live applications, modular designs of this aBL photodisinfection could be installed at critical AMR hotspots for decentralized advanced wastewater treatment. This can significantly unburden the load of contaminants in wastewater received by the WWTPs, and safeguarding aging and leaking pipeline systems. As urban WWTPs are currently ineffective at to fully remove pathogens, quaternary treatment of WWTP effluents for hygienization, are urgently required. Through this, the dissemination of AMR determinants through the wastewater system can be reduced, and ultimately lowing the risks for human and animal health. Targeted and innovative light-based on-site measures relieve downstream wastewater areas of AMR contamination, reducing their release into the environment (Mulani et al., 2019).

Since, it was initially a flow reactor for laboratory operation, in which the operating parameters were set to a maximum operating time of 4 h (equal to 26 min net irradiation), it can be assumed that an extension of the actual irradiation time would be even more effective. As the previously described (Section 2.2.) energy input of our flow aBL-reactor was already set to maximum. For optimization, this would be obtained by either increasing the irradiation time ($>$ 4 h) and/or reduce the total volume of liquid to be irradiated during circulation ($<$ 4 L total volume). Previous studies with static conditions where significantly longer irradiation times ($>$26 min) where achieved, support this hypothesis (Cong et al., 2023). To demonstrate this with a flow reactor, upscaling of the apparatus would be required. Decentralized modular inactivation technologies, such as aBL, would be the preferred intervention at AMR hotspots for combating AMR dissemination through sewage systems.

3.3. aBL irradiation induced DNA damages

Our goal was to determine whether aBL-mediated irradiation directly induces DNA lesions. The number of DNA damages per 10 kb length in bacteria before and after aBL irradiation, alone and combined with TMPyP or H_2O_2, was quantified via qPCR analyses. The qPCR amplification efficiency (E) and the correlation coefficients for each sample are presented in Table S5. The results (Fig. 6) show that aBL irradiation alone caused approximately 10 lesions per 10 kb DNA, while the combination with TMPyP and H_2O_2 resulted in about 13 and 12 lesions per 10 kb DNA, respectively. This indicates slightly higher DNA damage with TMPyP and H_2O_2 additions, though the overlapping error bars indicate no statistically significant difference between treatments.

More generally, aBL treatment itself is considered low risk for the development of bacterial resistance and tolerance due to its multitarget mode of action. This was studied by the tolerance (resistance development in *E. coli*, *K. pneumoniae*, and *P. aeruginosa* to aBL. The observed adaption was a stable feature (Rapacka-Zdonczyk et al., 2021). The impact of aBL in combination with TMPyP or H_2O_2 on the tolerance/

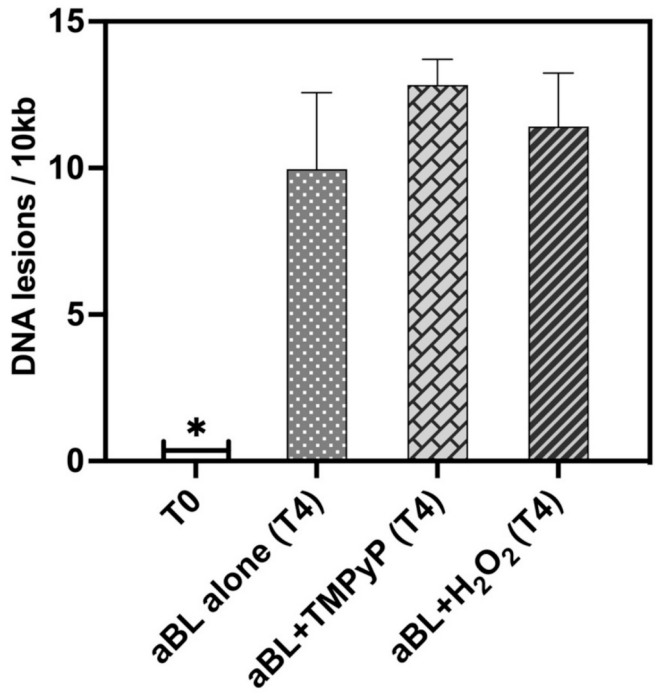

Fig. 6. DNA lesions per 10 kb DNA in the genomic DNA bacterial populations after aBL irradiation alone, or when combined either TMPyP or H_2O_2. Columns present averages of $n = 2$ lesion measurements after 4 h aBL irradiation (equal to 26 min effective irradiation). aBL treatments was performed using 420 nm LED lamps. The statistical significance is indicated by asterisks.

resistance development is so far not clarified. Nevertheless, we observed a direct or in direct impact on the DNA in bacteria. The resulting consequence will be studies in a following up project.

UV-C (100–289 nm) is widely used for (waste)water disinfection, with germicidal effects based on DNA, RNA, and protein absorption at specific wavelengths, causing molecular damage. The germicidal effect for many bacteria is achieved at near 254 nm, where DNA has its maximum absorption (Süß et al., 2009; Jungfer et al., 2007). Lethal damages, mainly thymine dimers, blocks DNA replication leading to reproductive cell death. UV-C-induced DNA lesions were quantified in a UV-C reactor used for drinking water treatment (113.9–114.5 mJ cm^{-2}), with up to 2–3 lesions per kilobase reported (Nocker et al., 2018). Bacteria have evolved molecular mechanisms, such as photoreactivation and dark repair systems, to restore such DNA lesions regulated by the *rec*A gene (Jungfer et al., 2007).

Opposed to UV inactivation, aBL irradiation activates ROS in the bacterial cells, targeting various cellular structures and causing lethal effects. Blue light can cause DNA damage either directly or indirectly. Lawrence et al. (2018) found that light at 385 nm induced cyclobutane pyrimidine dimers (CPDs), while 405 nm did not. ROS can target guanine bases in DNA, forming oxidized derivatives like 8-hydroxy-deoxyguanosine (8-OHdG). Yoshida et al. (2017) confirmed that singlet oxygen, a specific ROS, significantly increases 8-OHdG levels in bacterial cells exposed to aBL irradiation. However, there is limited information on whether aBL (405–460 nm) induces DNA lesions, requiring further investigation. Unlike UV-C which primarily causes nucleic acid alterations and bacteria during evolution developed DNA directed repair mechanisms against, until now no repair mechanisms are known to repair the manifold target structures impaired by aBL irradiation (Hadi et al., 2020). Thus, aBL combined with porphyrin photosensitizer is expected to be more sustainable.

Although our data does not imply direct DNA damage induced by aBL, it suggests that it induces indirect DNA damage through ROS generation. It yet remains uncertain whether *Eubacteria's* DNA repair mechanisms could regenerate damaged DNA. Given that aBL, especially with TMPyP, has multiple attack points, long-term DNA repair may not be effective. This suggests that aBL, particularly with TMPyP, poses a potent challenge for bacterial survival due to the compounded effects on cellular integrity. The extent to which DNA lesions affect regrowth after regeneration is a subject of future investigations. Increasing the energy input is relevant for enhancing the inactivation performance of aBL-induced processes for contaminated wastewater.

4. Conclusion

This study evaluated the potential and effectiveness of aBL irradiation at 405, 420, and 460 nm in deactivating ARB, FPB, and ARGs in wastewater effluents from AMR-contaminated WWTP. The reduction of ARB, FPB, and ARGs was examined under continuous-flow conditions using an aBL photoreactor, with and without the addition of TMPyP porphyrin photosensitizers or oxidative agent H_2O_2 to enhance the effect of aBL irradiation by up to five $\log_{10}$ units.

Among the investigated FPB targets, enterococci were more sensitive to aBL irradiation than *A. baumannii*, *P. aeruginosa*, and *E. coli*. Among the ARG targets, *ermB*, *tetM*, *sul1*, and bla_{VIM} were more sensitive to aBL irradiation, resulting in significant gene copy number reduction. Additionally, aBL irradiation induced DNA damage, leading to lesions in the genomic DNA of treated wastewater. These findings indicate that aBL irradiation enhanced with photosensitizer and the oxidative agent H_2O_2 is highly effective for inactivating FPB, ARB, and ARGs in wastewater. This approach shows promising for decentralized wastewater treatment at AMR hotspots, providing a viable solution for the mitigation AMR spread through sewage. Compared to static reactors, the energy input via parallel-connected aBL LED lamps in continuous-flow reactors is assumed to be significantly higher, resulting in more effective inactivation. Based on these promising aBL flow reactor results, approaches for optimizing up-scaling were indicated. Therefore, to enhance intracellular ROS generation and promote increased cell death, the aBL irradiation should have been combined with additional photosensitizers or oxidizing agents. Another possible optimization is the up-scaling of the aBL reactor, where stronger aBL intensities could be used for the treatment of contaminated wastewaters (i.e. more photoenergy, different LED lamps in parallel, etc). Such alterations would increase the effectiveness of aBL when used alone, without phosensitizer or oxidant addition. Future investigations should also explore the feasibility of adding photosensitizers or oxidizing agents to aBL treatments, and how this can be practically implemented in larger scale applications (with regard to recovery, regeneration, or immobilization).

CRediT authorship contribution statement

Xiaoyu Cong: Writing – original draft, Validation, Software, Methodology, Formal analysis. **Carsten Ulrich Schwermer:** Writing – review & editing, Visualization, Validation, Project administration, Data curation, Conceptualization. **Peter Krolla:** Visualization, Methodology, Investigation, Data curation. **Thomas Schwartz:** Writing – review & editing, Supervision, Project administration, Methodology, Funding acquisition.

Consent to participate

Not applicable.

Consent for publication

Not applicable.

Ethics approval

This study did not need etical approval.

Funding

We thank the JPI-AMR initiative and the German BMBF-DLR for financial support within the framework of the HOTMATS project.

Declaration of competing interest

The authors declare that they have no known competing financial interests or personal relationships that could have appeared to influence the work reported in this paper.

Acknowledgement

We acknowledge support by the JPI AMR, BMBF-DLR, and KIT as well as the local wastewater treatment plant operators, which provide the wastewater and conventionally treated samples. Further thanks go to all project partners which were involved the acquiring of the analysed samples.

Data availabilitys

Data are available from the corresponding author upon reasonable request.

Appendix A. Supplementary data

Supplementary data to this article can be found online at https://doi.org/10.1016/j.scitotenv.2025.179208.

Data availability

Data will be made available on request.

References

Ahmed, S.K., Hussein, S., Qurbani, K., Ibrahim, R.H., Fareeq, A., Mahmood, K.A., Mohamed, M.G., 2024. Antimicrobial resistance: impacts, challenges, and future prospects. J. Med. Surg. Publ. Health 2, 100081.

Alexander, J., Hembach, N., Schwartz, T., 2020. Evaluation of antibiotic resistance dissemination by wastewater treatment plant effluents with different catchment areas in Germany. Sci. Rep. 10 (1), 8952.

Alexander, J., Hembach, N., Schwartz, T., 2022. Identification of critical control points for antibiotic resistance discharge in sewers. Sci. Total Environ. 820, 153186.

Ayrapetyan, M., Williams, T., Oliver, J.D., 2018. Relationship between the viable but nonculturable state and antibiotic persister cells. J. Bacteriol. 200 (20), 10–1128.

Barber, J.L., 2015. Using Blue Light for Bacterial Inactivation. Master's thesis, Lancaster University (United Kingdom).

Cong, X., Krolla, P., Khan, U.Z., Savin, M., Schwartz, T., 2023. Antibiotic resistances from slaughterhouse effluents and enhanced antimicrobial blue light technology for wastewater decontamionation. Environ. Sci. Pollut. Res. 30 (50), 109315–109330.

Cong, X., Mazierski, P., Miodyńska, M., Zaleska-Medynska, A., Horn, H., Schwartz, T., Gmurek, M., 2024. The role of TiO2 and gC3N4 bimetallic catalysts in boosting antibiotic resistance gene removal through photocatalyst assisted peroxone process. Sci. Rep. 14 (1), 22897.

Dannenmann, B., Lehle, S., Lorscheid, S., Huber, S.M., Essmann, F., Schulze-Osthoff, K., 2017. Simultaneous quantification of DNA damage and mitochondrial copy number by long-run DNA-damage quantification (LORD-Q). Oncotarget 8 (68), 112417.

Enwemeka, C., Baker, T., Bumah, V., 2021. The role of UV and blue light in photo-eradication of microorganisms. J. Photochem. Photobiol. 8, 100064.

Gao, P., Munir, M., Xagoraraki, I., 2012. Correlation of tetracycline and sulfonamide antibiotics with corresponding resistance genes and resistant bacteria in a conventional municipal wastewater treatment plant. Sci. Total Environ. 421, 173–183.

Garcez, A.S., Núnez, S.C., Baptista, M.S., Daghastanli, N.A., Itri, R., Hamblin, M.R., Ribeiro, M.S., 2011. Antimicrobial mechanisms behind photodynamic effect in the presence of hydrogen peroxide. Photochem. Photobiol. Sci. 10, 483–490.

Guan, Y.H., Chen, J., Chen, L.J., Jiang, X.X., Fu, Q., 2020. Comparison of UV/H2O2, UV/PMS, and UV/PDS in destruction of different reactivity compounds and formation of bromate and chlorate. Front. chem. 8, 581198.

Hadi, J., Wu, S., Brightwell, G., 2020. Antimicrobial blue light versus pathogenic bacteria: mechanism, application in the food industry, hurdle technologies and potential resistance. Foods 9, 1895. https://doi.org/10.3390/foods9121895.

Hazra, M., Durso, L.M., 2022. Performance efficiency of conventional treatment plants and constructed wetlands towards reduction of antibiotic resistance. Antibiotics 11 (1), 114. https://doi.org/10.3390/antibiotics11010114.

Hazra, M., Watts, J.E., Williams, J.B., Joshi, H., 2024. An evaluation of conventional and nature-based technologies for controlling antibiotic-resistant bacteria and antibiotic-resistant genes in wastewater treatment plants. Sci. Total Environ. 917, 170433.

Hembach, N., Schmid, F., Alexander, J., Hiller, C., Rogall, E.T., Schwartz, T., 2017. Occurrence of the mcr-1 colistin resistance gene and other clinically relevant antibiotic resistance genes in microbial populations at different municipal wastewater treatment plants in Germany. Front. Microbiol. 8.

Hembach, N., Alexander, J., Hiller, C., Wieland, A., Schwartz, T., 2019. Dissemination prevention of antibiotic resistant and facultative pathogenic bacteria by ultrafiltration and ozone treatment at an urban wastewater treatment plant. Sci. Rep. 9 (1), 12843.

Hembach, N., Bierbaum, G., Schreiber, C., Schwartz, T., 2022. Facultative pathogenic bacteria and antibiotic resistance genes in swine livestock manure and clinical wastewater: a molecular biology comparison. Environ. Pollut. 313, 120128.

Herraiz-Carboné, M., Cotillas, S., Lacasa, E., de Baranda, C.S., Riquelme, E., Cañizares, P., Sáez, C., 2021. A review on disinfection technologies for controlling the antibiotic resistance spread. Sci. Total Environ. 797, 149150.

Huang, S., Lin, S., Qin, H., Jiang, H., Liu, M., 2023. The parameters affecting antimicrobial efficiency of antimicrobial blue light therapy: a review and prospect. Biomedicines 11 (4), 1197.

Idil, O., Darcan, C., Ozkanca, R., 2011. The effect of UV-A and different wavelengths of visible lights on survival of salmonella typhimurium in seawater microcosms. J. Pure Appl. Microbiol. 5 (2), 581–592.

Jungfer, C., Schwartz, T., Obst, U., 2007. UV-induced dark repair mechanisms in bacteria associated with drinking water. Water Res. 41 (1), 188–196.

Lawrence, K.P., Douki, T., Sarkany, R.P., Acker, S., Herzog, B., Young, A.R., 2018. The UV/visible radiation boundary region (385–405 nm) damages skin cells and induces "dark" cyclobutane pyrimidine dimers in human skin in vivo. Sci. Rep. 8 (1), 12722.

Leanse, L.G., Dos Anjos, C., Mushtaq, S., Dai, T., 2022. Antimicrobial blue light: a 'magic bullet' for the 21st century and beyond? Adv. Drug Deliv. Rev. 180, 114057.

MacIsaac, S.A., Reid, B., Ontiveros, C., Linden, K.G., Stoddart, A.K., Gagnon, G.A., 2024. UV LED wastewater disinfection: the future is upon us. Water Res. X 24, 100236.

Maclean, M., MacGregor, S.J., Anderson, J.G., Woolsey, G., 2009. Inactivation of bacterial pathogens following exposure to light from a 405-nanometer light-emitting diode array. Appl. Environ. Microbiol. 75 (7), 1932–1937.

Maldonado-Carmona, N., Ouk, T.S., Leroy-Lhez, S., 2022. Latest trends on photodynamic disinfection of gram-negative bacteria: Photosensitizer's structure and delivery systems. Photochem. Photobiol. Sci. 1–33.

Mathur, A., Parihar, A.S., Modi, S., Kalra, A., 2023. Photodynamic therapy for ESKAPE pathogens: an emerging approach to combat antimicrobial resistance (AMR). Microb. Pathog. 106307.

Mishra, S., Imlay, J., 2012. Why do bacteria use so many enzymes to scavenge hydrogen peroxide? Arch. Biochem. Biophys. 52 (2), 145–160.

Mulani, M.S., Kamble, E.E., Kumkar, S.N., Tawre, M.S., Pardesi, K.R., 2019. Emerging strategies to combat ESKAPE pathogens in the era of antimicrobial resistance: a review. Front. Microbiol. 10, 539.

Mušković, M., Planinić, M., Crepulja, A., Lušić, M., Glad, M., Lončarić, M., Gobin, I., 2023. Photodynamic inactivation of multidrug-resistant strains of *Klebsiella pneumoniae* and *Pseudomonas aeruginosa* in municipal wastewater by tetracationic porphyrin and violet-blue light: the impact of wastewater constituents. PLoS One 18 (8), e0290080.

Ngo, V.N., Truong, T.N.T., Tran, T.T., Nguyen, L.T., Mach, N.B., Vu, V.V., Vu, T.M., 2023. A combination of blue light at 460 nm and H_2O_2 for the safe and effective eradication of *Staphylococcus aureus* in an infected mouse skin abrasion model. Microorganisms 11 (12), 2946.

Nocker, A., Shah, M., Dannenmann, B., Schulze-Osthoff, K., Wingender, J., Probst, A.J., 2018. Assessment of UV-C-induced water disinfection by differential PCR-based quantification of bacterial DNA damage. J. Microbiol. Methods 149, 89–95.

O'Neil, J., 2014. Review on Antibiotic Resistance: Tackling a Crisis for the Health and Wealth of Nations. Heal Wealth Nations.

Rapacka-Zdonczyk, A., Wozniak, A., Kruszewska, B., Waleron, K., Grinholc, M., 2021. Can gram-negative bacteria develop resistance to antimicrobial blue light treatment? Int. J. Mol. Sci. 22, 11579.

Sah, S.K., Hemalatha, S., 2015. Extended spectrum Beta lactamase (ESBL) mechanism of antibiotic resistance and epidemiology. Int. J. Pharmtech. Res. 7 (2), 303–309.

Savin, M., Alexander, J., Bierbaum, G., Hammerl, J.A., Hembach, N., Schwartz, T., Kreyenschmidt, J., 2021. Antibiotic-resistant bacteria, antibiotic resistance genes, and antibiotic residues in wastewater from a poultry slaughterhouse after conventional and advanced treatments. Sci. Rep. 11 (1), 16622.

Sib, E., Voigt, A.M., Wilbring, G., Schreiber, C., Faerber, H.A., Skutlarek, D., Schmithausen, R.M., 2019. Antibiotic resistant bacteria and resistance genes in biofilms in clinical wastewater networks. Int. J. Hyg. Environ. Health 222 (4), 655–662.

Sib, E., Lenz-Plet, F., Barabasch, V., Klanke, U., Savin, M., Hembach, N., Bierbaum, G., 2020. Bacteria isolated from hospital, municipal and slaughterhouse wastewaters show characteristic, different resistance profiles. Sci. Total Environ. 746, 140894.

Süß, J., Volz, S., Obst, U., Schwartz, T., 2009. Application of a molecular biology concept for the detection of DNA damage and repair during UV disinfection. Water Res. 43 (15), 3705–3716.

Truong, H.B., Huy, B.T., Ray, S.K., Lee, Y.I., Cho, J., Hur, J., 2020. H_2O_2-assisted photocatalysis for removal of natural organic matter using nanosheet C3N4-WO3 composite under visible light and the hybrid system with ultrafiltration. Chem. Eng. J. 399, 125733.

Uluseker, C., Kaster, K.M., Thorsen, K., Basiry, D., Shobana, S., Jain, M., Pala-Ozkok, I., 2021. A review on occurrence and spread of antibiotic resistance in wastewaters and

in wastewater treatment plants: mechanisms and perspectives. Front. Microbiol. 12, 717809.
Wainwright, M., 1998. Photodynamic antimicrobial chemotherapy (PACT). J. Antimicrob. Chemother. 42 (1), 13–28.
Wang, J., Chen, X., 2020. Removal of antibiotic resistance genes (ARGs) in various wastewater treatment processes: an overview. Crit. Rev. Environ. Sci. Technol. 52 (4), 571–630. https://doi.org/10.1080/10643389.2020.1835124.
Wang, Y., Han, Y., Li, L., Liu, J., Yan, X., 2022. Distribution, sources, and potential risks of antibiotic resistance genes in wastewater treatment plant: a review. Environ. Pollut. 310, 119870.
Wen, Q., Yang, L., Duan, R., Chen, Z., 2016. Monitoring and evaluation of antibiotic resistance genes in four municipal wastewater treatment plants in Harbin, Northeast China. Environ. Pollut. 212, 34–40.
WHO, 2019. No time to wait: securing the future from drug-resistant infections. Artforum Int. 54, 113–114.
Woźniak, A., Grinholc, M., 2022. Combined antimicrobial blue light and antibiotics as a tool for eradication of multidrug-resistant isolates of Pseudomonas aeruginosa and *Staphylococcus aureus*: *in vitro* and *in vivo* studies. Antioxidants 11 (9), 1660.
Yoon, H., Kim, H.C., Kim, J., You, K., Cho, Y., Kim, S., 2022. Toxicity impact of hydrogen peroxide on the fate of zebrafish and antibiotic resistant bacteria. J. Environ. Manag. 302, 114072.
Yoshida, A., Sasaki, H., Toyama, T., Araki, M., Fujioka, J., Tsukiyama, K., Yoshino, F., 2017. Antimicrobial effect of blue light using *Porphyromonas gingivalis* pigment. Sci. Rep. 7 (1), 5225.
Zhu, S., Coffman, J.A., 2017. Simple and fast quantification of DNA damage by real-time PCR, and its application to nuclear and mitochondrial DNA from multiple tissues of aging zebrafish. BMC. Res. Notes 10, 1–6.